frontiers | Frontiers in Earth Science

TYPE Original Research
PUBLISHED 10 April 2024
DOI 10.3389/feart.2024.1368326

OPEN ACCESS

EDITED BY
Hu Li,
Southwest Petroleum University, China

REVIEWED BY
Denglin Han,
Yangtze University, China
Jinbu Li,
Chinese Academy of Sciences (CAS), China
Tao Luo,
The University of Queensland, Australia

*CORRESPONDENCE
Ruyue Wang,
wry1990@vip.qq.com
Yuejiao Liu,
lyj523029007@qq.com

RECEIVED 10 January 2024
ACCEPTED 26 March 2024
PUBLISHED 10 April 2024

CITATION
Wang R, Liu Y, Li Z, Wang D, Wang G, Lai F, Li Z and He J (2024), Microscopic pore structure characteristics and controlling factors of marine shale: a case study of Lower Cambrian shales in the Southeastern Guizhou, Upper Yangtze Platform, South China.
Front. Earth Sci. 12:1368326.
doi: 10.3389/feart.2024.1368326

Microscopic pore structure characteristics and controlling factors of marine shale: a case study of Lower Cambrian shales in the Southeastern Guizhou, Upper Yangtze Platform, South China

Ruyue Wang[1,2,3,4,5]*, Yuejiao Liu[4]*, Zhi Li[1,2,3], Dahai Wang[1,2,3], Guanping Wang[1,2,3], Fuqiang Lai[4], Zhihao Li[1,2,3] and Jianhua He[5]

[1]State Key Laboratory of Shale Oil and Gas Enrichment Mechanisms and Efficient Development, Beijing, China, [2]Sinopec Key Laboratory of Shale Oil/Gas Exploration and Production Technology, Beijing, China, [3]Sinopec Petroleum Exploration and Production Research Institute, Beijing, China, [4]Chongqing Key Laboratory of Complex Oilfield Exploration and Development, Chongqing University of Science and Technology, Chongqing, China, [5]College of Energy, Chengdu University of Technology, Chengdu, China

A systematic study of the pore structure characteristics of Lower Cambrian shales in the southeastern Upper Yangtze Platform, was conducted using organic geochemistry, mineralogy, nitrogen adsorption, physical property analysis, and scanning electron microscopy. The results indicate that: 1) The Total organic carbon (TOC) content shows a strong correlation with quartz and clay minerals. Shales with low TOC content and rich in clay minerals primarily exhibit slit-shaped and narrow slit-like inter-clay particle pores with pore size distribution is dominated by mesopores and macropores. Shales with high TOC content predominantly feature narrow slit-like and ink bottle-shaped pores with pore size distribution dominated by micropores and mesopores. 2) Shale pore structures vary significantly under different gas content and preservation conditions. Shales under favorable preservation conditions exhibit a relatively "high porosity, low permeability, and high gas content" pattern, with well-developed organic pores and a strong pore-permeability correlation. In contrast, shales under unfavorable preservation conditions appear dense, with excessively developed fractures increasing both average pore size and local permeability. The pore-permeability correlation is weak, presenting a relatively "low porosity, high permeability, and low gas content" pattern. 3) TOC content plays a crucial role in controlling pore structure, showing overall positive correlations with pore volume, specific surface area, and porosity, and negative correlations with pore size. High TOC content enhances shale plasticity, resulting in lower pore diameters. Factors such as compaction and unfavorable preservation conditions lead to the shrinkage, collapse, and closure of some narrow pore throats, negatively impacting pore volume, specific surface area, brittleness, and fractal dimension, exhibiting a negative correlation with TOC content. 4) The pore structure of Lower Cambrian shales is complex, with

fractal dimensions D_1 and D_2 exhibiting negative correlations with average pore size and positive correlations with TOC, specific surface area, and total pore volume. A high D_1 value indicates well-preserved nanoscale pore surface structures with low complexity, suggesting minimal alteration by external fluids and better shale gas preservation. D_1 serves as an indicator for shale gas content and preservation conditions. D_2 shows better correlations with various pore structure parameters, making it suitable for characterizing pore structures.

KEYWORDS

pore structure, fractal dimension, preservation condition, Niutitang Formation, Bianmachong Formation, Lower Cambrian, South China

1 Introduction

Shale oil and gas, as an important supplement and replacement for conventional oil and gas resources, have become a global exploration and development hotspot. Shale gas is generated and stored in organic-rich mud shale formations, constituting a natural gas accumulation system with adsorption and free gas as its main occurrence modes (Hu et al., 2021; Wang et al., 2022). The discovery of the Fuling Shale Gas Field marks a significant breakthrough in China's shale gas exploration and development, playing a crucial role in leading and demonstrating unconventional oil and gas development and optimizing the energy structure in China. In recent years, with technological advancements and the rise of nanogeoscience (Wang et al., 2021a), research on the micro-pore structure of shale reservoirs has become a key focus in both domestic and international shale oil and gas exploration and development. As research deepens and new technologies emerge, there has been substantial progress in understanding shale micro-pore structures (Bernard et al., 2012; Wang et al., 2017; Zhu et al., 2019; Hackley et al., 2020; Xu et al., 2021; Sun M. et al., 2022; Sun Y. et al., 2022; Li et al., 2022).

Studies by Yang et al. (2016) and Wang et al. (2018) on the Longmaxi Formation in the Sichuan Basin revealed a positive correlation between organic matter abundance and shale pore volume and specific surface area. Liu et al. (2016), in their research on the micro-pore structure of Longmaxi Formation shale in southern Sichuan during the Lower Silurian period, found that approximately 80% of the shale reservoir space consists of micro- to mesopores. Poorly organic-rich shales are dominated by slit-shaped pores with a fractal dimension generally less than 2.75, and the storage space is mainly inorganic mineral pores. Conversely, richly organic shales primarily feature "ink bottle" shaped pores with a fractal dimension generally greater than 2.85, and the storage space is mainly organic pores. Zhang et al. (2020), in their study of Longmaxi Formation shale in Weiyuan area, suggested that the fractal dimension is mainly related to the degree of micro-pore development. Specifically, Total Organic Carbon (TOC) and quartz content control micro-pore development and show a positive correlation with the fractal dimension, while the volume fractions of carbonate rocks and clay minerals are negatively correlated with the fractal dimension.

The characteristics of shale reservoirs are collectively controlled by organic matter (OM), inorganic mineral composition, their evolution, and diagenetic processes. The pore characteristics of shale reservoirs vary significantly under different geological conditions, exhibiting strong heterogeneity (Aplin et al., 2006; Bernard et al., 2012; Wang et al., 2018; Dowey and Taylor, 2020; Liu Y. et al., 2021; Wang et al., 2021a; Liu D. et al., 2021; Sun M. et al., 2022; Lai et al., 2022; Wang et al., 2023a; Wang et al., 2023b; Dong et al., 2023; Shi et al., 2023). Additionally, influenced by the unique geological conditions in China, shale gas in southern marine shale formations is significantly constrained by preservation conditions (Wang et al., 2016; Liu D. et al., 2021; Guo et al., 2022; Wu et al., 2022). The development characteristics and controlling factors of shale pores in different thermal evolution stages and under the influence of tectonic preservation conditions are still not clear enough, and research on the response and constraints of shale pore structures to gas content and preservation conditions in southern China is still an area that requires further exploration (Wang et al., 2021a; 2022). This study focuses on the Lower Cambrian Niutitang Formation and Bianmachong Formation shales in the southeast part of the Yangtze region, aiming to provide insights for the exploration and development of Paleozoic ancient shale gas in complex tectonic regions in southern China and similar areas worldwide.

2 Geological setting

The study area is located at the southeastern margin of the Upper Yangtze Block. In the Early Cambrian, it experienced passive continental margin deep-water shelf sedimentation, with water depth gradually decreasing from southeast to northwest (Wang et al., 2017; Wei et al., 2022). The majority of the block comprises Cambrian sedimentary strata, with a total thickness ranging from 2,000 to 2,700 m. Organic-rich shales are mainly developed in the Lower Cambrian Niutitang Formation, Jiumenchong Formation, and Bianmachong Formation (Chen et al., 2020). In the study area, the Niutitang Formation shale exhibits significant thickness (50–70 m) and a widespread distribution in the Cengong block, predominantly consisting of black/gray-black siliceous shale. The Bianmachong Formation represents a suite of continental margin, relatively close to offshore, and shallow-water restricted marine-land source clastic sediments (Chen et al., 2020). It displays characteristics of both marine shale (sedimentary environment) and transitional shale (lithological composition), with predominant interbedding of gray-black shales and shale with thin interlayers of fine sand-siltstone. The maximum thickness of a single shale layer in the formation is 35.5 m.

3 Samples and methods

A total of 52 shale samples were collected from the Niutitang Formation and Bianmachong Formation in the study area, including TXA well, CYA well, and TMA well (Figure 1). In this study, a series of tests, analyses, and calculations were conducted on these 52 black shale samples, including Total Organic Carbon (TOC) content, maturity, mineral composition, organic geochemistry, Field Emission Scanning Electron Microscopy (FE-SEM), petrophysical properties, pore structure, methane isotherm adsorption, and fractal dimension analysis. All sample analyses were performed by SGS North America Inc. (Beijing) using unconventional oil and gas technology. The TOC content of the 52 samples was measured using a LECO CS-230 carbon-sulfur analyzer, following the guidelines of "GB/T 19,145-2003 Determination of Total Organic Carbon in Sedimentary Rocks." The asphaltene reflectance (R_b) of 9 samples was determined using an MPV-III microscope photometer, based on the method outlined in "SY/T 5124-1995 Method for Determination of Vitrinite Group Reflectance in Sedimentary Rocks." The equivalent vitrinite reflectance (R_o) was calculated using the formula Ro = 0.3195 + 0.679R_b (Feng and Chen, 1988). Mineral composition analysis of 22 samples was conducted using a SmartLab9 X-ray diffractometer, following the guidelines of "SY/T 5163-2010 X-ray Diffraction Analysis of Clay Minerals and Common Non-Clay Minerals in Sedimentary Rocks." The pore volume and permeability of 52 samples were measured using an HKC-2 helium porosity tester, according to "SY/T 5336-2006." Nitrogen adsorption experiments and pore structure parameter analysis of 22 samples were performed using a Quadrasorb SI specific surface area and pore size analyzer, following the method outlined in "SY/T 6154-1995 Static Nitrogen Adsorption Capacity Method for Determining Rock Specific Surface Area and Pore Size Distribution." Scanning electron microscopy observations of 22 samples were conducted using a Quanta 200F FE-SEM at a temperature of 24°C and a humidity level of 35%. Shale gas content testing was conducted using the WX-1 integrated intelligent shale on-site desorption instrument developed by Wuxi Research Institute of Petroleum Geology, Sinopec Petroleum Exploration and Production Research Institute. The gas loss recovery method was based on the USBM method (Yang et al., 2022). In addition, this paper provides a comprehensive and systematic observation and description of shale fractures, including the measurement of the following metrics: 1) fracture type; 2) fracture inclination angle; and 3) fracture linear density (frequency of fracture occurrence per unit length).

Characterization by fractal dimension has been widely used to quantitatively describe pore surface roughness and the pore structure of heterogeneous porous media, and the FHH model presently is the most effective fractal model for studying pore structure of porous materials (Avnir and Jaroniec, 1989). Thus, the FHH model is used to describe the fractal characteristics of pore structure of shales in the study area. There are two distinct linear segments at a relative pressure (P/P_0) of 0–0.5 and 0.5–1, indicating that the pore spaces in shale have fractal characteristics in these two regions. Accordingly, the fractal dimension D_1 (P/P_0: 0–0.5) and D_2 (P/P_0: 0.5–1.0) are used to characterize the roughness of the pore surface and the complexity of the pore structure, respectively.

4 Results

4.1 Geochemical and mineral composition characteristics

The Total Organic Carbon (TOC) content of black shale samples from the Lower Cambrian in the study area ranges from 0.5% to 8.5%, with the equivalent vitrinite reflectance (R_o) ranging between 2.2% and 2.9%, indicating an over-mature stage. Specifically, the TOC content of the Bianmachong Formation shale mainly falls within the range of 0.5%–1.7%, while the Niutitang Formation shale exhibits TOC content ranging from 1.1% to 8.5%, with the majority exceeding 4% (Table 1). Regarding mineral composition, both the Bianmachong Formation and Niutitang Formation black shale are dominated by quartz and clay minerals (Table 1). The Bianmachong Formation shale has a quartz content ranging from 33.1% to 38.4%, with an average of 36.2%, and a relatively high clay mineral content ranging from 44.4% to 54.9%. In comparison, the Niutitang Formation shale has a higher quartz content ranging from 27.5% to 68.3%, with an average of 47.7%, and a clay mineral content ranging from 8.7% to 42.5%, with an average of 21.8%. The averages for feldspar, pyrite, and carbonate minerals are 11.5%, 10.1%, and 8.9%, respectively. There is a strong positive correlation between TOC content and the presence of quartz and clay minerals (Figure 2), indicating a close relationship between TOC and quartz. Shale intervals rich in TOC show elevated biogenic quartz content (Wang et al., 2017).

4.2 Physical properties and gas content

The statistical results of shale physical parameters (Table 2) indicate that the physical properties and gas content of Niutitang and Bianmachong shale formations are generally comparable. However, significant differences in pore volume are observed under different gas content and preservation conditions. Taking Niutitang Formation as an example, the average gas content in TXA well is 1.6 m^3/t, with methane accounting for over 80%. In CYA well, the average gas content is 1.0 m^3/t, with methane exceeding 95%. TMA well generally exhibits gas content below 0.3 m^3/t, with nitrogen accounting for over 95% (Wang et al., 2016). The gas content and preservation conditions in TXA, CYA, and TMA wells of the Niutitang Formation gradually deteriorate, and the porosity decreases accordingly (Table 2; Figure 3). In terms of permeability, the permeability of the Bianmachong and Niutitang shale in TX-1 well, which has better preservation and gas content, is generally below 2×10^{-3} mD, showing a good positive correlation between pore and permeability (Figure 3). On the other hand, the permeability of Niutitang shale in CYA and TMA wells is higher, with a weaker correlation between pore and permeability. Compared to TXA well, TMA well's Niutitang shale exhibits a smaller median radius, higher median pressure, denser reservoir, and generally demonstrates a "low porosity, high permeability, low gas content" characteristic. In contrast, the shale properties of TXA well, characterized by better preservation and gas content, generally show a "high porosity, low permeability, high gas content" pattern (Table 2; Figure 3).

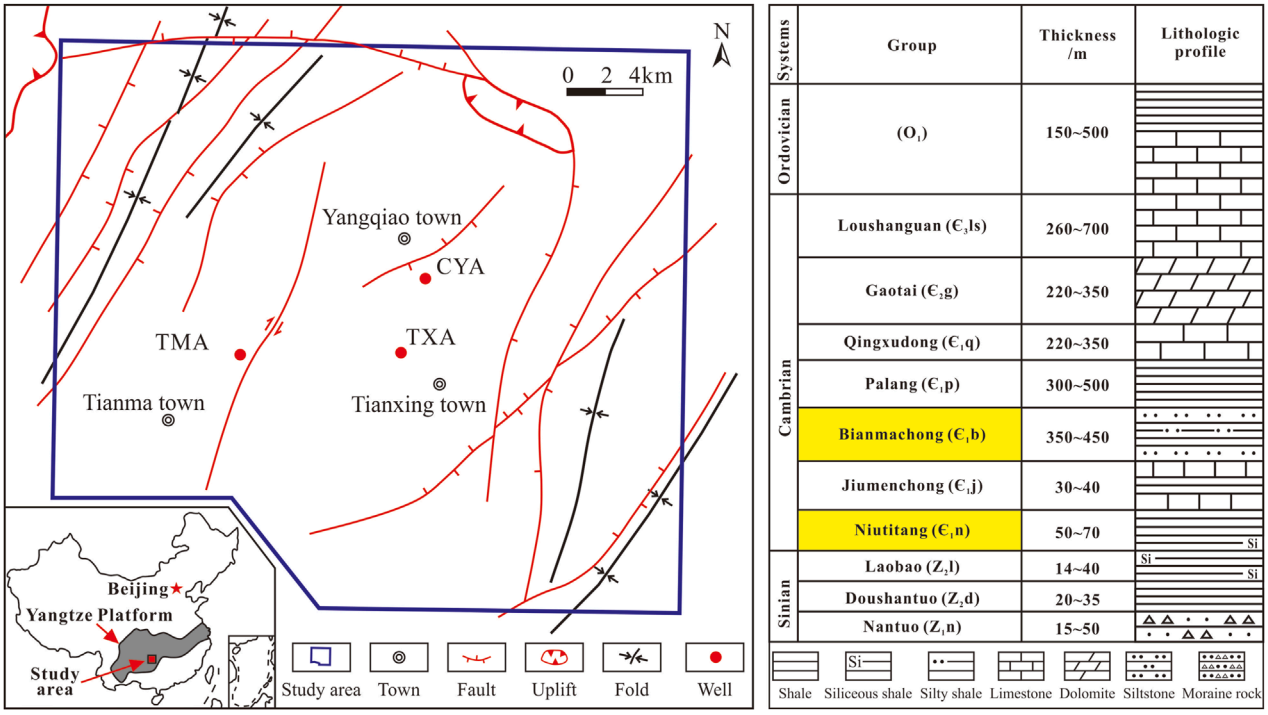

FIGURE 1
Location and stratigraphic characteristics of the study area.

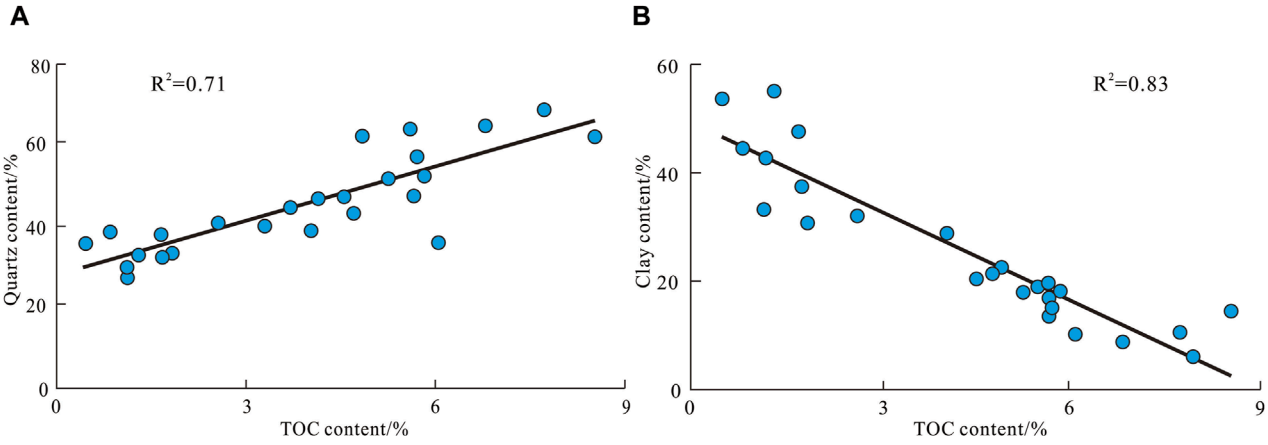

FIGURE 2
Correlations between TOC and mineral contents in Lower Cambrian shale. **(A)** Correlations between TOC and quartz content. **(B)** Correlations between TOC and clay mineral content.

4.3 Pore structure characteristics

4.3.1 Pore types

According to the classification by the International Union of Pure and Applied Chemistry (IUPAC) (Sing, 1985), nitrogen adsorption isotherms of 22 shale samples exhibit three types of curves: H2, H3, and H4 (Figures 4A–C), corresponding to ink bottle-shaped, slit-shaped, and narrow slit-like pores, respectively. The adsorption curves and corresponding pore types and parameter statistics are shown in Table 3. Clay-rich, organic-poor shales are dominated by slit-shaped pores, with a larger average pore diameter and lower pore volume and specific surface area. Organic-rich shales, on the other hand, are characterized by ink bottle-shaped and narrow slit-like pores, with a smaller average pore diameter and higher pore volume and specific surface area.

In comparison with the Lower Silurian Longmaxi Formation shale in southern China, the Lower Cambrian shale exhibits a lower degree of organic pore development and smaller pore sizes (Wang et al., 2017; 2018; Zhang et al., 2022). The average pore diameter is generally less than 4–5 nm (Table 3), and the nitrogen

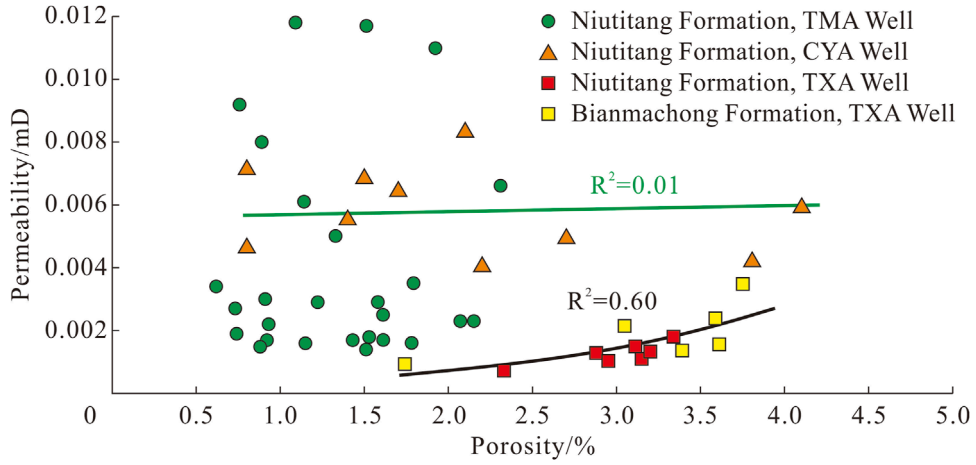

FIGURE 3
Characteristics of shale physical properties under different gas contents and preservation conditions.

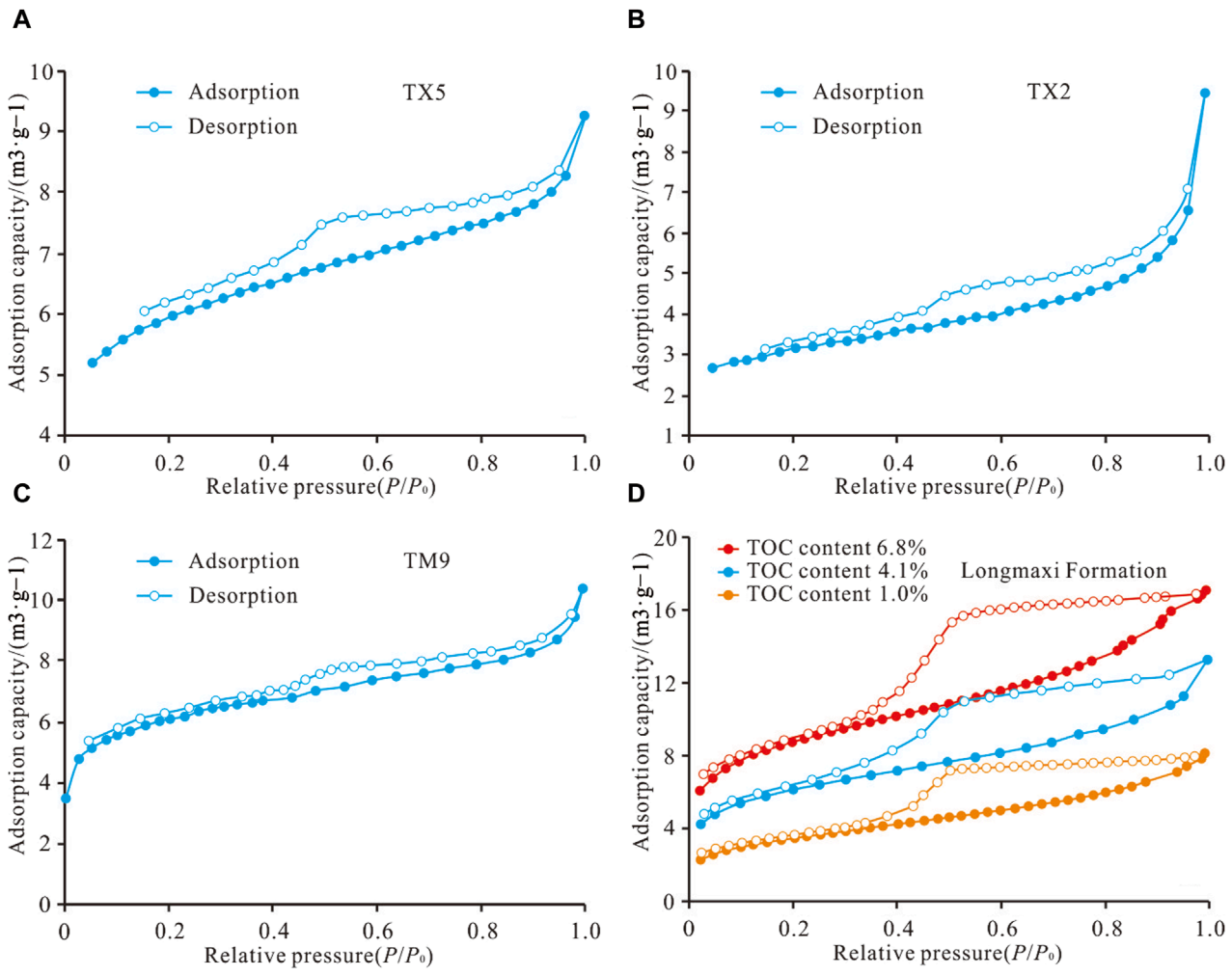

FIGURE 4
Shale Nitrogen Adsorption Isotherm Characteristics. **(A–C)** Liquid nitrogen adsorption and desorption isotherms of Cambrian shale samples. **(D)** Liquid nitrogen adsorption and desorption isotherms of Silurian Longmaxi shale samples (Yang et al., 2016).

TABLE 1 Statistical summary of TOC, maturity, and mineral composition parameters for Lower Cambrian shale.

Sample number	Depth/m	Formation	TOC content/%	Equivalent R_o/%	Quartz/%	Clay/%	Feldspar/%	Pyrite/%	Carbonate/%	Fractal dimension D_1	Fractal dimension D_2
TX1	1,451.9	Bianmachong	0.81	2.3	38.4	44.4	10.6	1.9	1.7	2.716	2.836
TX2	1,512.4		1.66	2.6	37.6	47.1	8.4	4.4	2.6	2.768	2.801
TX3	1,591.0		1.30	2.5	33.1	54.9	6.5	5.5	/	2.715	2.716
TX4	1,709.4		0.45	2.2	35.5	53.5	5.7	5.4	/	2.627	2.593
TX5	1,783.3	Niutitang	5.80	2.8	52.7	17.9	9.5	12.1	7.8	2.821	2.935
TX6	1,791.2		6.77	2.9	64.0	8.7	8.1	10.7	8.5	2.828	2.941
TX7	1,800.2		6.04	2.5	35.9	10.2	27.2	12.9	13.8	2.840	2.949
TM1	1,453.7		7.68	/	68.3	10.3	8.6	6.8	6.2	2.755	2.952
TM2	1,461.8		5.63	/	47.6	13.8	14.6	12.4	11.7	2.738	2.940
TM3	1,406.1		1.10	/	27.5	33.0	8.5	8.9	22.1	2.603	2.776
TM4	1,409.6		1.12		30.0	42.5	8.0	10.1	9.4	2.564	2.757
TM5	1,417.6		1.70	/	32.5	37.5	11.4	15.0	3.6	2.634	2.792
TM6	1,421.4		1.77	2.3	33.0	30.5	12.7	12.7	11.1	2.684	2.855
TM7	1,423.4		2.56	/	40.5	31.4	13.1	10.8	4.0	2.651	2.842
TM8	1,428.8		4.00	/	39.0	28.9	10.5	8.9	12.7	2.726	2.920
TM9	1,441.6		5.61	/	64.0	16.7	4.6	5.1	10.0	2.728	2.910
TM10	1,451.3		8.50	/	62.0	14.2	10.8	6.7	7.0	2.753	2.934
TM11	1,457.3		5.23	/	51.6	17.7	13.5	8.7	8.5	2.742	2.919
TM12	1,466.8		4.52	/	47.5	20.5	14.0	13.5	4.5	2.715	2.919
TM13	1,470.1		4.68	2.4	43.3	21.3	11.8	14.0	9.6	2.736	2.929
TM14	1,480.8		4.80	/	61.8	21.9	9.7	6.6	/	2.769	2.921
TM15	1,482.8		5.68	/	57.0	15.1	9.6	6.7	9.6	2.783	2.930

10.3389/feart.2024.1368326

TABLE 2 Statistics of shale reservoir physical parameters in the study area.

Well name	Formation	Porosity/%	Permeability/ 10^{-3} mD	Gas content/ (m^3/t)	Median radius/μm	Median pressure/ MPa	Maximum pore throat radius/μm
TXA	$\epsilon_1 b$	(1.7–3.8)/3.3 (6)	(1.4–4.3)/2.3 (6)	(0.3–1.3)/1.0 (6)	(0.12–0.19)/0.14 (12)	(3.9–6.3)/5.3 (12)	(0.47–0.94)/0.67 (12)
	$\epsilon_1 n$	(2.3–3.3)/3.0 (7)	(0.7–1.8)/1.3 (7)	(0.9–2.8)/1.6 (14)	(0.15–0.20)/0.17 (7)	(3.6–5.1)/4.5 (7)	(0.62–0.94)/0.73 (7)
CYA	$\epsilon_1 n$	(0.8–4.1)/1.8 (10)	(4.1–8.4)/5.9 (10)	(0.2–4.5)/1.0 (12)	/	/	/
TMA	$\epsilon_1 n$	(0.6–2.3)/1.3 (29)	(1.4–13.7)/4.8 (29)	(0.1–0.3)/0.2 (33)	(0.02–0.12)/0.05 (15)	(6.2–38.6)/23.2 (15)	(0.35–1.03)/0.73 (15)

Note: (Min ~ Max)/Mean (Number of Samples).

TABLE 3 Pore types and parameter statistics of shale pores.

Curve type	Pore type	Sample number	Average TOC/%	Average pore diameter/nm	Average pore volume/ (10^{-3} cm^3/g)	Average specific surface area/(m^2/g)	Ration (%)
H2	Ink bottle	TM1, TM6, TX5, TX6, TX7	5.6	3.0	14.1	19.6	22.7
H3	Slit-shaped	TM3, TM4, TM5, TX1, TX2, TX4	1.1	5.7	11.0	8.9	27.3
H4	Narrow slit-like	TM2, TM7, TM8, TM9, TM10, TM11, TM12, TM13, TM14, TM15, TX3	4.7	3.5	13.9	18.8	50.0

adsorption quantity and hysteresis loop area are significantly smaller than those of the Longmaxi Formation (Figure 4D), indicating that the Longmaxi Formation has larger pore volume and more ink bottle-shaped organic pores (Liu et al., 2016).

4.3.2 Microscopic characteristics of pores

Microscopic features of shale under scanning electron microscopy reveal that the clay-rich shale of the Bianmachong Formation has a low TOC content, with well-developed interlayer pores between slit-shaped clay minerals (Figure 5A), corresponding to the morphology of adsorption isotherms, which are predominantly slit-shaped and narrow slit-like (Table 3). In comparison with the Bianmachong Formation, the Niutitang Formation shale has a higher TOC content, and the development of organic matter (OM) pores has increased, but the pore size of OM pores is generally less than 50 nm (Figures 5A–C). In contrast to the TXA well, the Niutitang Formation shale in the TMA well, which has poor preservation conditions, is denser, with smaller organic pore sizes (Figures 5B, C). The shale exhibits high levels of compression and deformation, with densely developed fractures, and noticeable phenomena of particle and aggregate compression and fragmentation, resulting in incomplete and irregular shapes (Figures 5D, E). Additionally, in the Niutitang Formation shale from the TMA well, narrow fissures between OM and mineral particles, formed either by OM shrinkage or mineral fracture, are commonly observed (Figure 5F). This is consistent with the predominant narrow slit-like morphology of pores corresponding to the N_2 adsorption isotherms of shale samples from the TMA well (Table 3).

4.3.3 Fractal dimensions

Fractal characteristics of shale pores (Table 1) show that the fractal dimension D_1 of Lower Cambrian shale ranges from 2.564 to 2.840, with a mean value of 2.723. The D_2 dimension ranges from 2.593 to 2.952, with a mean value of 2.867. D_2 is generally greater than D_1, indicating that the internal structure of the shale is significantly more complex than its surface structure. Both D_1 and D_2 are markedly greater than those of Longmaxi Formation shale in the Sichuan Basin and its surrounding areas, suggesting a higher complexity in the pore structure of the Lower Cambrian shale.

As shown in Figure 6, there is a negative correlation between clay mineral content and fractal dimensions (Figures 6A, D). The positive correlation of TOC with quartz content in marine shale makes the relationships between quartz, TOC, and fractal dimensions similar

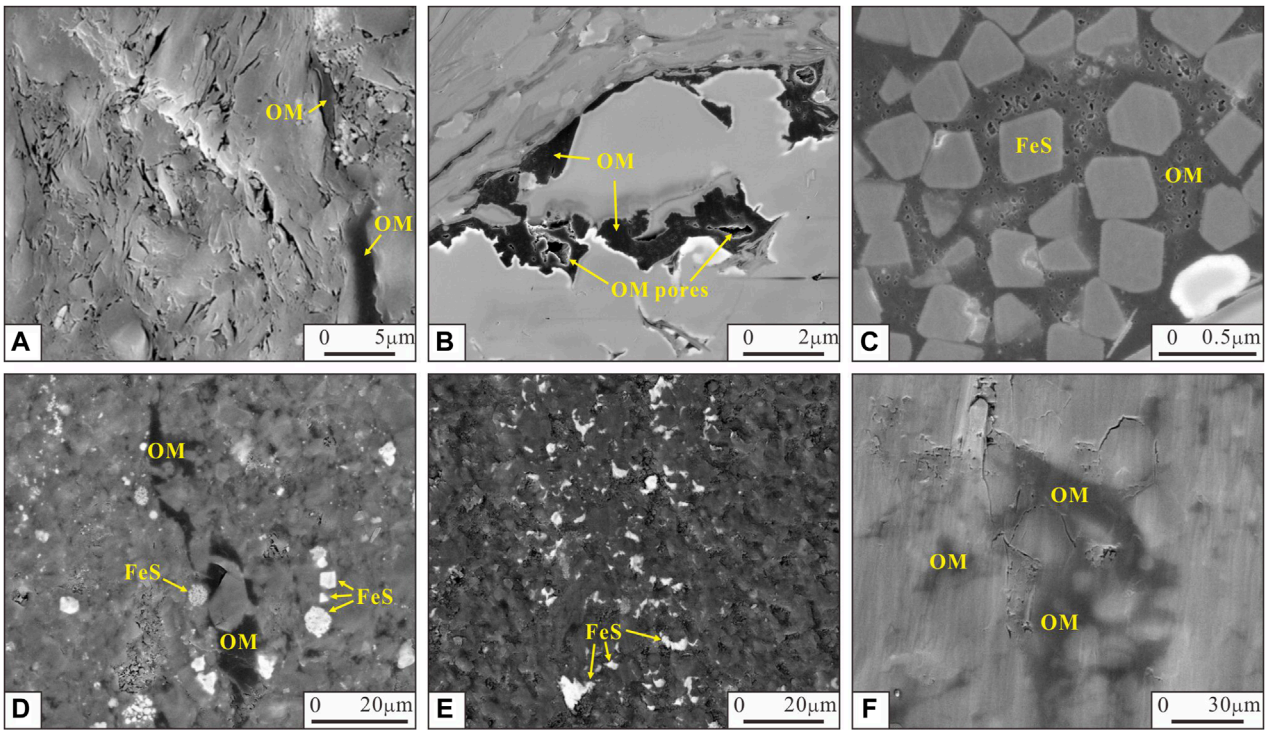

FIGURE 5
FE-SEM images of Lower Cambrian shale in the study area. **(A)** Well-developed interlayer pores between slit-shaped clay minerals are more prominent than OM pores, Bianmachong Formation, TXA well, 1,718.4 m. **(B)** Lower development of OM pores, Niutitang Formation, TXA well, 1,800.2 m. **(C)** OM pore sizes generally smaller than 20–50 nm, Niutitang Formation, TMA well, 1,450.5 m. **(D)** Microscopic features show well-preserved particle and aggregate shapes, particularly regular forms of pyrite (FeS) particles, Niutitang Formation, TXA well, 1,779.3 m. **(E)** Microscopic features reveal dense reservoir, with noticeable compression and fragmentation of pyrite (FeS) particles and aggregates, Niutitang Formation, TMA well, 1,445.3 m. **(F)** Low development of OM pores, narrow fissures developed at the edges of OM and minerals, Niutitang Formation, TMA well, 1,439.3 m.

to those of reservoir parameters (Figures 6B, C, E, F). Overall, the correlations between TOC, quartz content, clay minerals, and D_2 are better than those with D_1. It is noteworthy that with increasing TOC content, especially when TOC content exceeds 4%, the increase in fractal dimensions D_1 and D_2 is limited and tends to stabilize. Additionally, when TOC content exceeds 6%, a slight decrease in fractal dimensions D_1 and D_2 is observed with the increasing TOC content (Figures 6C, F).

The relationship between D_1 and D_2 and pore structure parameters reveals a negative correlation with average pore diameter and a positive correlation with specific surface area and total pore volume (Figure 7). Elevated values of D_1 and D_2 indicate the development of nanoscale pores, suggesting increased surface roughness and internal structural complexity. Generally, D_2 demonstrates stronger correlations with various pore structure parameters (Figures 7D–F). As D_2 increases, shale pore diameter gradually decreases, while pore volume and specific surface area increase. When D_2 surpasses 2.9, its variation with pore volume and specific surface area becomes limited, indicating stabilization in pore structure and complexity. Additionally, samples from TXA well with better gas content and preservation conditions exhibit significantly larger D_1 than samples from TMA well under the same conditions (Figures 6A–C, 7A–C), implying that shale pore surfaces in TXA well are notably rougher than those in TMA well.

5 Discussion

5.1 Impact of TOC content and mineral composition on pore structure

Interrelationships among shale pore structure parameters reveal a strong positive correlation between total pore volume and specific surface area, both of which are negatively correlated with average pore diameter (Figures 8J–L). Compared to the Bianmachong Formation shale, the Niutitang Formation shale has a smaller average pore diameter but larger specific surface area and pore volume (Figures 8A–C). In terms of the relationships between TOC, quartz, clay mineral content, and specific surface area, pore volume, and average pore diameter, the variations in reservoir pore structure parameters are primarily controlled by the positive correlation of TOC and quartz content. Specifically, average pore diameter is negatively correlated with TOC and quartz content but positively correlated with clay mineral content (Figures 8G–I). Specific surface area and total pore volume generally exhibit positive correlations with TOC and quartz content but negative correlations with clay mineral content (Figures 8D–F). Shales with low organic content (TOC content less than 2%) typically have a specific surface area less than 10 m^2/g, while shales with high organic content (TOC content greater than 2%) generally exhibit an

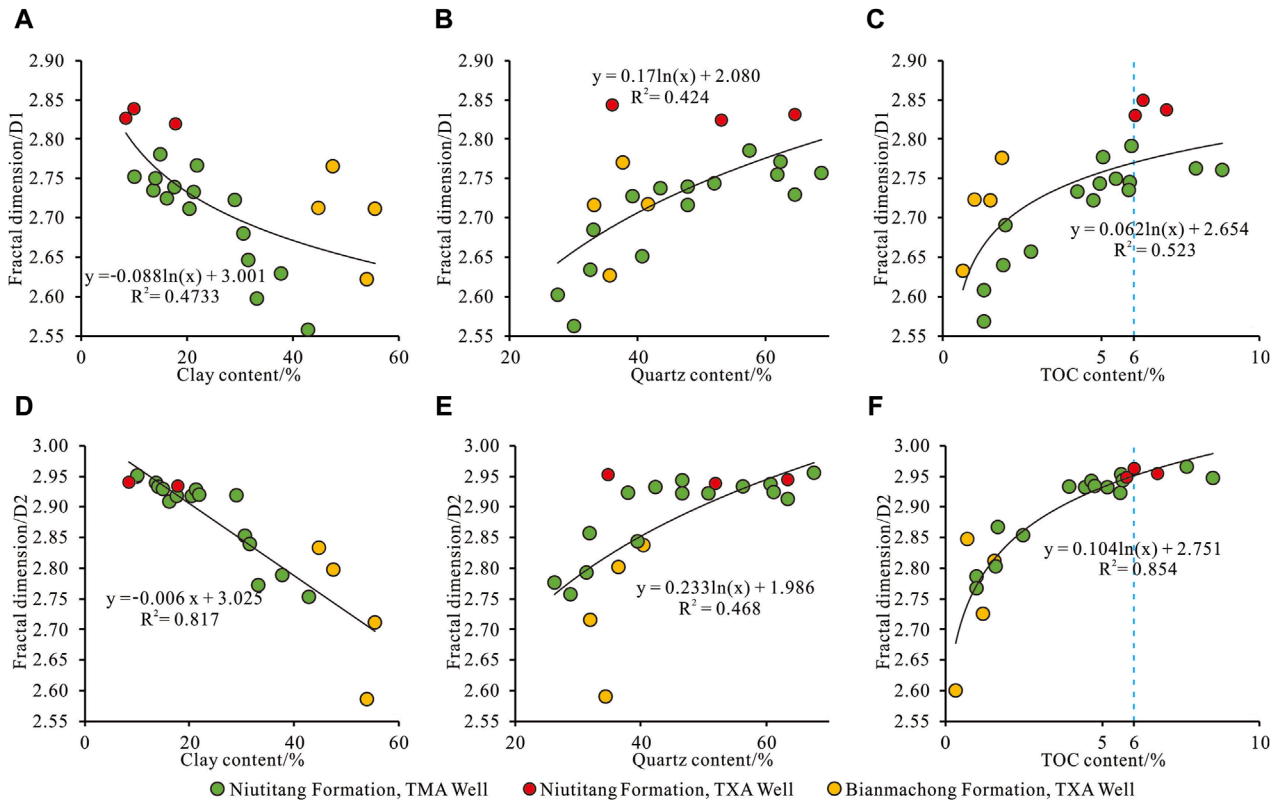

FIGURE 6
Correlations between fractal dimensions and reservoir parameters of shale. **(A)** Correlation between clay mineral content and fractal dimension D1. **(B)** Correlation between quartz content and fractal dimension D1. **(C)** Correlation between TOC content and fractal dimension D1. **(D)** Correlation between clay mineral content and fractal dimension D2. **(E)** Correlation between quartz content and fractal dimension D2. **(F)** Correlation between TOC content and fractal dimension D2.

average pore diameter less than 3–4 nm and a specific surface area greater than 20 m^2/g (Figures 8D, G). This indicates the abundant development of organic pores smaller than 5 nm within organic matter (Kuila et al., 2014; Wang et al., 2017), leading to a reduction in average pore diameter and an increase in specific surface area and pore volume, facilitating the adsorption of gases (Mosher et al., 2013). An anomalous decrease in specific surface area and total pore volume occurs when TOC and quartz content are excessively high (Figures 8A, B, D, E).

When the TOC content reaches 4%, the fractal dimensions D_1 and D_2 generally exceed 2.7 and 2.9, respectively, with a limited increase and a tendency to stabilize (Figures 6C, F). The pore structures exhibit similarity and convergence, indicating a stabilization of the pore structure. Studies by Vernik and Landis (1996) have shown that when the TOC content in shale exceeds 5%, organic matter between clay and detrital particles can form a continuous network structure, isolating clay and detrital particles from each other and stabilizing the shale pore structure. Therefore, when the TOC content is above 4%, the uniformity of shale pore development is high, dominated by organic pores and a small number of pores between clay mineral particles.

In the Niutitang Formation shale of the study area, the relationship between TOC content and porosity, as well as rock mechanical parameters, also exhibits a segmented pattern. When the TOC content is around 6.0% or higher, the relationship between TOC content and porosity, as well as elastic modulus, changes from positive correlation to negative correlation (Figure 9). This indicates that excessively high TOC content enhances shale plasticity (Milliken et al., 2013; Wang et al., 2017), leading to shrinkage and closure of some pores under compaction (Wang et al., 2017). The aforementioned relationships highlight the significant control of TOC and quartz content on shale reservoir pore structure. The coupling relationship between TOC, quartz content, and shale porosity, pore volume, specific surface area, fractal dimensions, and brittleness suggests a geological and engineering sweet spot in high-TOC and high-quartz content shale intervals that have not yet reached the TOC inflection point. For shale intervals with excessively high TOC content, such as the Niutitang Formation shale with TOC content exceeding 6%, the negative correlation between TOC content and average pore diameter, increased plasticity, and changes in pore structure parameters indicate a decreasing trend in porosity, pore volume, specific surface area, fractal dimensions, and brittleness (Figures 6C, F, 8A). This trend is unfavorable for the accumulation of shale gas and reservoir fracturing enhancements. Therefore, identifying the key parameters and their critical values controlling shale reservoir pore structure is of great significance for shale gas exploration and development.

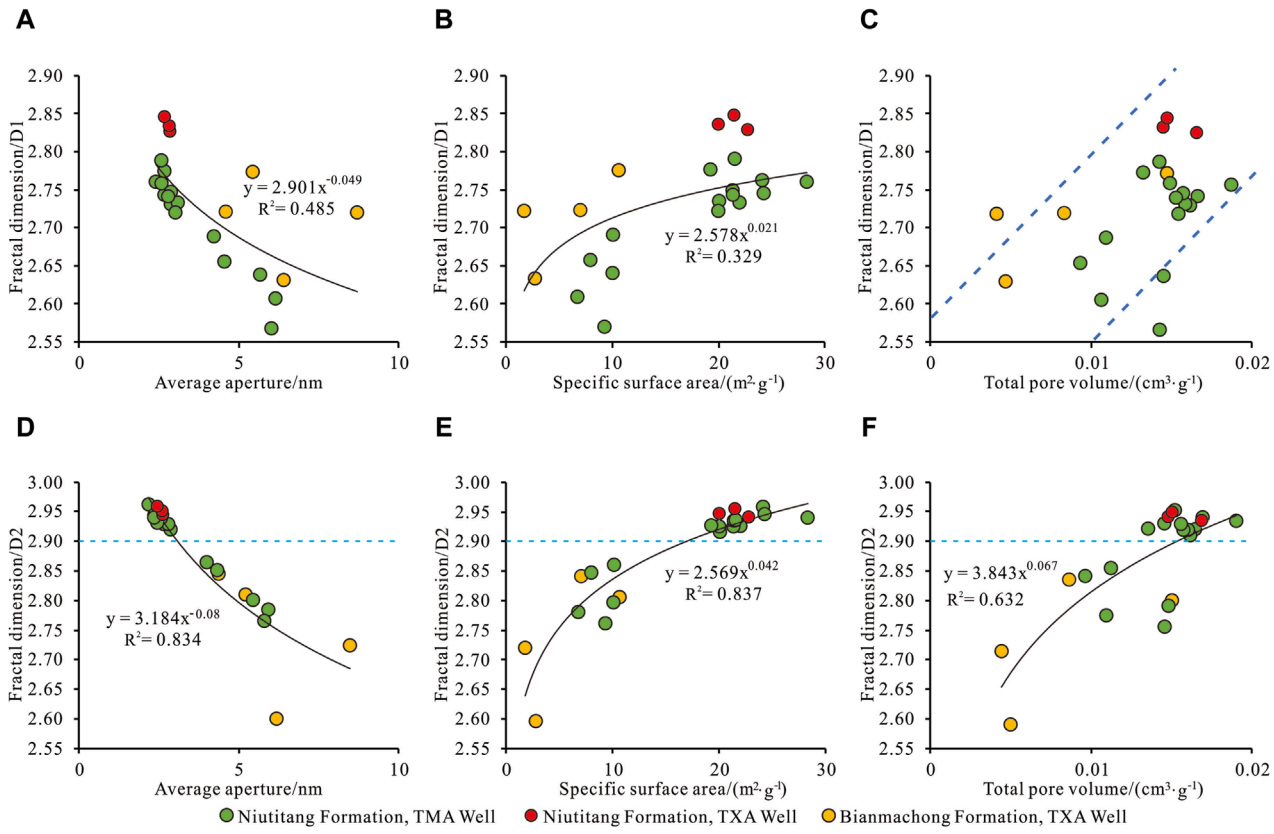

FIGURE 7
Correlations between fractal dimensions and pore structure parameters. **(A)** Correlation between pore size and fractal dimension D1. **(B)** Correlation between specific surface area and fractal dimension D1. **(C)** Correlation between total pore volume and fractal dimension D1. **(D)** Correlation between pore size and fractal dimension D2. **(E)** Correlation between specific surface area and fractal dimension D2. **(F)** Correlation between total pore volume and fractal dimension D2.

5.2 Impact of tectonic preservation conditions on pore structure and gas content

The tectonic preservation conditions are significant factors influencing shale gas enrichment and are closely related to the development of faults and fractures. Practical exploration and development of shale gas in southern China indicate that, influenced by multiple tectonic movements, shale fractures vary in degrees of development across different regions and stratigraphic units, exerting a crucial influence on the accumulation and preservation of shale gas (Wang et al., 2016; 2021b; Fan et al., 2020; 2024). The development scale of high-angle fractures often reflects the preservation conditions of shale gas, showing a strong correlation with shale brittleness. This fracture type is predominant in marine shale formations in southern China (Wang et al., 2021b).

There are noticeable differences in porosity and gas content under different preservation conditions in the Niutitang Formation. The drilling results of three wells in the study area (Figure 10) reveal that the TXA well is located in a structurally stable area, distant from faults, and the drilling operation proceeded smoothly. The shale gas content of the Niutitang Formation shale ranges from 1.1 to 2.9 m^3/t, with a maximum of 7.1 m^3/t. The CYA well is situated near a fault, experiencing four instances of lost circulation during the drilling of the shallow 500 m carbonate rock. The gas content ranges from 0.3 to 1.8 m^3/t. The TMA well is located in a strike-slip fault zone with highly developed highcarbonate rock. The gas content-angle faults and fractures. Numerous and large-scale high-angle fractures are encountered, and gas anomalies appear shortly after drilling into shallow layers. The on-site desorption gas content is only 0.1–0.3 m^3/t, with nitrogen (N_2) constituting over 95% of the gas composition, indicating that the shale gas preservation conditions of the TMA well have been significantly compromised (Wang et al., 2016). The relationship between fracture density and gas content in three wells in the study area is illustrated in Figure 10. The moderately developed fractures in the TXA well contribute to an increase in shale content. As the scale of fracture development increases, preservation conditions gradually deteriorate, leading to a decrease in gas content in CYA and TMA wells. Therefore, excessive fracture development disrupts shale gas preservation conditions, introducing external fluids. Under the influence of fractures and foreign fluids, the local permeability of shale increases, resulting in a weaker pore-permeability correlation overall, characterized by "low porosity, high permeability, low gas content" (Table 2; Figure 3).

The characteristics of N_2 adsorption-desorption isotherms also reflect differences in pore structure under different preservation conditions. Under the same geological conditions, the area of N_2 adsorption-desorption hysteresis loop corresponds well to

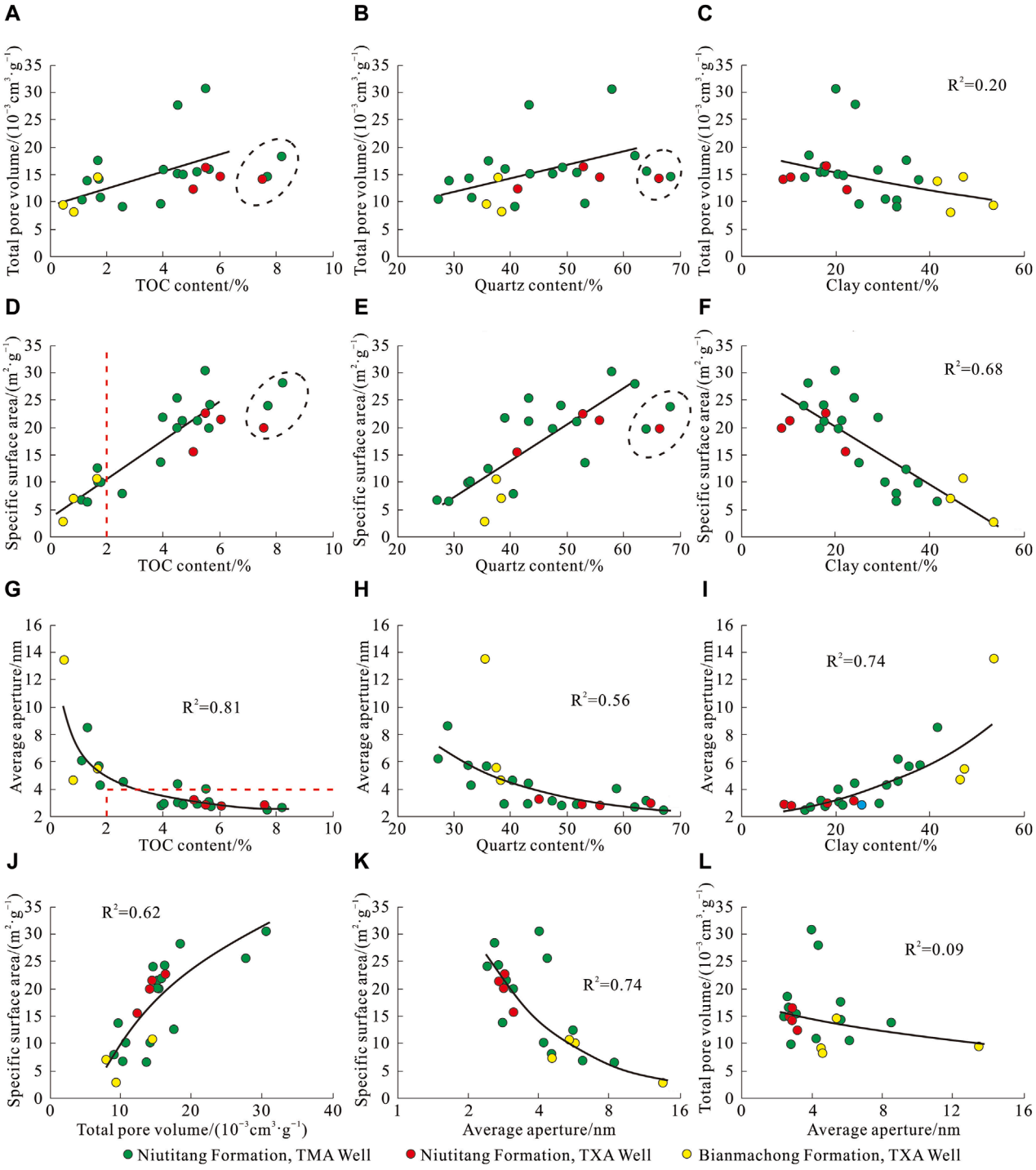

FIGURE 8
Correlations among TOC, mineral content and pore structure parameters. **(A)** Correlation between total pore volume and TOC content. **(B)** Correlation between total pore volume and quartz content. **(C)** Correlation between total pore volume and clay mineral content. **(D)** Correlation between specific surface area and TOC content. **(E)** Correlation between specific surface area and quartz content. **(F)** Correlation between specific surface area and clay mineral content. **(G)** Correlation between pore size and TOC content. **(H)** Correlation between pore size and quartz content. **(I)** Correlation between pore size and clay mineral content. **(J)** Correlation between total pore volume and specific surface area. **(K)** Correlation between pore size and specific surface area. **(L)** Correlation between pore size and total pore volume.

TOC content, representing the development of organic pores. In shale from TXA well with good gas content and preservation conditions, the area of N_2 adsorption-desorption hysteresis loop is significantly larger than in TMA well. The dominant pore type in TXA well is ink bottle-shaped organic pores, while TMA well exhibits predominantly narrow slit-like pores (Table 3). This phenomenon reflects that marine organic-rich shale reservoir spaces are primarily dominated by ink bottle-shaped organic pores. With

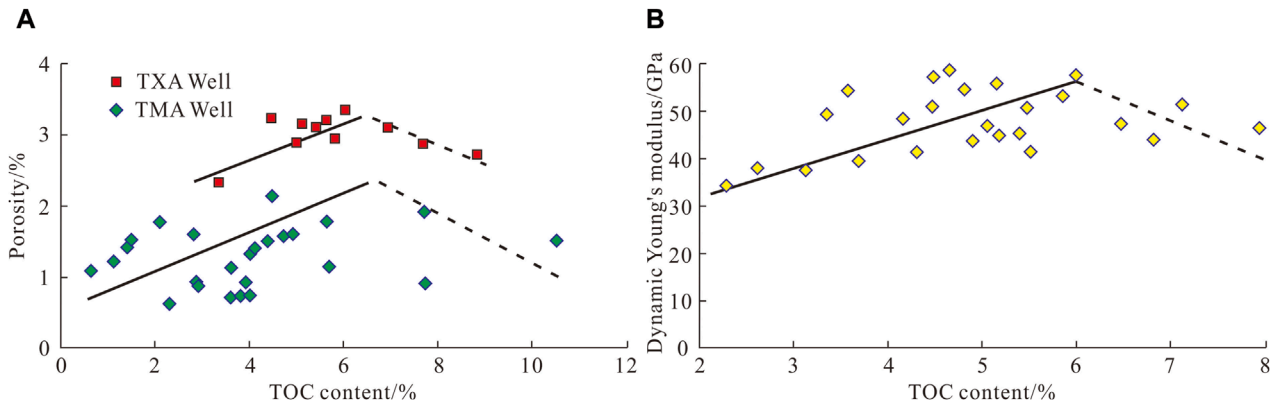

FIGURE 9
(A) Correlation between TOC content and porosity in the Niutitang shale. **(B)** Correlation between TOC content and dynamic Young's modulus in the Niutitang shale of well TX1.

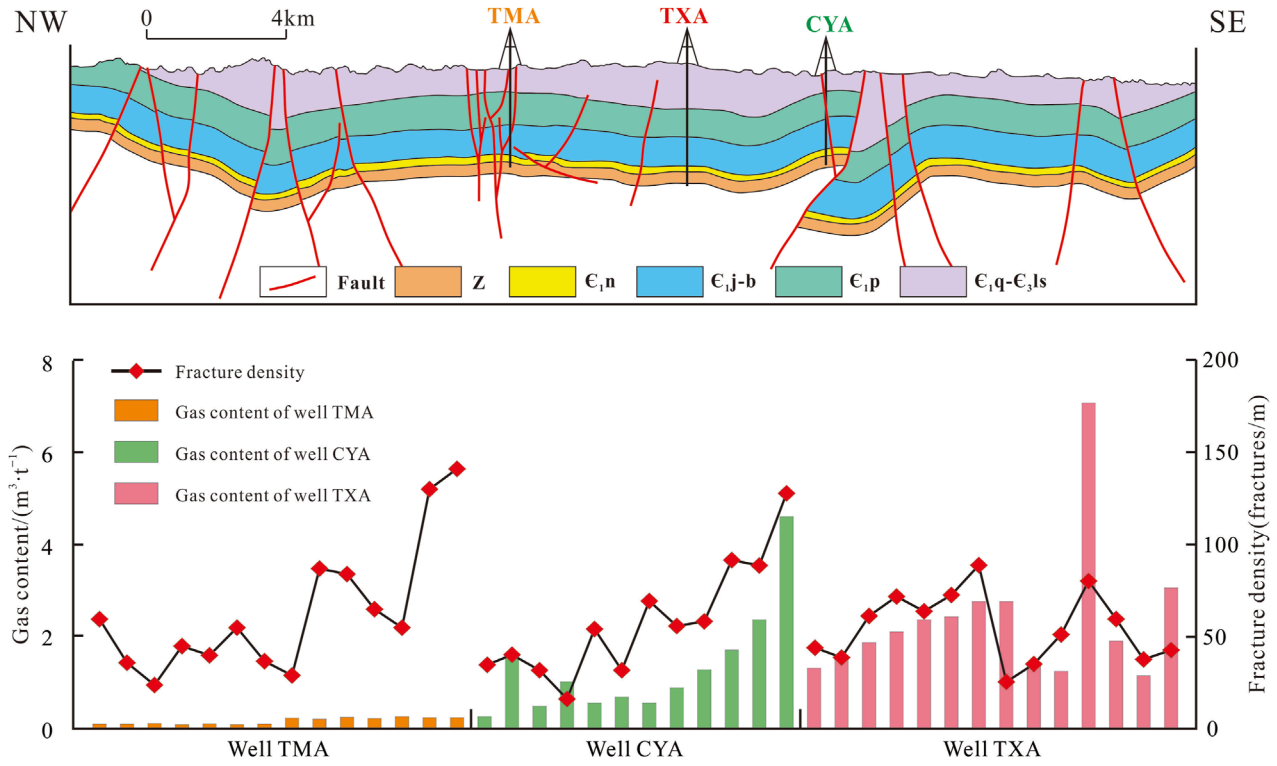

FIGURE 10
Structural position, fracture density, and gas content distribution of key wells in the Niutitang shale of the study area.

the deterioration of preservation conditions, decrease in formation pressure, and the escape of shale gas, organic pores gradually contract and close, and the proportion of slit-shaped pores between clay mineral particles in the storage space increases.

The relationship between fractal dimensions D_1 and D_2 and pore structure parameters indicates that both D_1 and D_2 play a certain indicative role in the development of nanoscale pores. High values of D_1 and D_2 suggest that the pore surface roughness and internal structure are complex, and the pores have not undergone external fluid alteration. Excessive fracture development and unfavorable preservation conditions in the TMA well result in varying degrees of alteration in shale pore structure, especially in pore surface structure. This alteration leads to a reduction in pore surface roughness, consequently causing a significant decrease in the fractal dimension D_1 compared to the TXA well samples (Figures 6A–C, 7A–C). Therefore, fractal dimension D_2 is suitable for characterizing the pore structure of shale, while fractal dimension D_1 reflects the degree of alteration of the pore structure. Both dimensions are crucial indicators of gas content and preservation conditions in shale, especially in structurally complex areas.

6 Conclusion

(1) In the Lower Cambrian shale of the southeastern Guizhou, there is a strong correlation between TOC content and quartz and clay minerals. Low-TOC, clay-rich shale primarily exhibits platy and slit-shaped interlayer pores dominated by mesopores and macropores, with pore sizes generally larger than 5 nm. Organic-rich shale, on the other hand, features mainly slit-shaped and ink bottle-shaped pores, with a pore size distribution primarily in the micropore and mesopore range, generally smaller than 4 nm. The specific surface area of organic-rich shale is 2–3 times that of clay-rich shale. Total pore volume and specific surface area are positively correlated, and clay content is positively correlated with average pore size. However, the correlations between total pore volume/specific surface area and clay mineral content/average pore size are negative.

(2) Significant differences in pore structure are observed in shale reservoirs under different gas contents and preservation conditions. Shale under favorable preservation conditions exhibits a relatively "high porosity, low permeability, and high gas content" feature, with higher pore volume and peak pore size and a well-developed organic pore network, leading to strong pore-permeability correlation. In contrast, shale reservoirs under unfavorable preservation conditions appear denser, with lower pore volume and peak pore size. Shrinkage and compaction of organic matter induce the development of contraction fractures, and excessive fracture development increases average pore size and local permeability. The pore-permeability correlation is weak, resulting in a "low porosity, high permeability, and low gas content" characteristic.

(3) TOC content plays a crucial role in controlling pore structure and shale brittleness. It is generally positively correlated with pore volume, specific surface area, and pore density, and negatively correlated with average pore size. Shale sections with excessively high TOC content exhibit enhanced plasticity, lower pore sizes, and factors such as compaction or unfavorable preservation conditions cause some narrow pores to shrink, collapse, and close. This results in negative correlations between TOC content and pore volume, pore density, specific surface area, brittleness, and fractal dimensions. Therefore, identifying key parameters and their critical values that control shale reservoir pore structure is essential for shale gas exploration and development.

(4) The pore structure of Lower Cambrian shale is complex, with fractal dimensions D_1 and D_2 negatively correlated with average pore size and positively correlated with TOC, specific surface area, and total pore volume. D_2 exhibits better correlations with various pore structure parameters and is suitable for characterizing shale pore structure. D_1 serves as an indicator of gas content and preservation conditions, with high D_1 values indicating well-maintained nanoscale pore surface structure and complexity, less affected by external fluid alteration, and conducive to shale gas preservation.

Data availability statement

The original contributions presented in the study are included in the article/Supplementary material, further inquiries can be directed to the corresponding authors.

Author contributions

RW: Conceptualization, Data curation, Formal Analysis, Funding acquisition, Investigation, Methodology, Project administration, Resources, Software, Supervision, Validation, Visualization, Writing–original draft, Writing–review and editing. YL: Writing–original draft, Writing–review and editing. ZhL: Writing–original draft, Writing–review and editing. DW: Writing–original draft, Writing–review and editing. GW: Writing–original draft, Writing–review and editing. FL: Writing–original draft, Writing–review and editing. ZaL: Writing–original draft, Writing–review and editing. JH: Writing–original draft, Writing–review and editing.

Funding

The author(s) declare that financial support was received for the research, authorship, and/or publication of this article. This research was funded by the Sinopec Ministry of Science and Technology Project (No. 21042-3).

Conflict of interest

The authors declare that the research was conducted in the absence of any commercial or financial relationships that could be construed as a potential conflict of interest.

Publisher's note

All claims expressed in this article are solely those of the authors and do not necessarily represent those of their affiliated organizations, or those of the publisher, the editors and the reviewers. Any product that may be evaluated in this article, or claim that may be made by its manufacturer, is not guaranteed or endorsed by the publisher.

References

Aplin, A. C., Matenaar, I. F., McCarty, D. K., and van der Pluijm, B. A. (2006). Influence of mechanical compaction and clay mineral diagenesis on the microfabric and pore-scale properties of deep-water Gulf of Mexico mudstones. *Clays Clay Min.* 54, 500–514. doi:10.1346/CCMN.2006.0540411

Avnir, D., and Jaroniec, M. (1989). An isotherm equation for adsorption on fractal surfaces of heterogeneous porous materials. *Langmuir* 5 (6), 1431–1433. doi:10.1021/la00090a032

Bernard, S., Wirth, R., Schreiber, A., Schulz, H.-M., and Horsfield, B. (2012). Formation of nanoporous pyrobitumen residues during maturation of the barnett shale (fort worth basin). *Int. J. Coal Geol.* 103, 3–11. doi:10.1016/j.coal.2012.04.010

Chen, P., Lin, W., Gong, D., Shang, F., and Liu, X. (2020). Sedimentary geochemical characteristics and its sedimentary environment significance of the black shale of the Lower Cambrian Bianmachong Formation in the Cen'gong block, Guizhou Province. *Chin. J. Geol.* 55 (4), 1025–1043. doi:10.12017/dzkx.2020.063

Dong, T., Kang, L., Zhang, Y., and Gao, Y. (2023). Pore fractal characteristics of lacustrine shale of upper cretaceous nenjiang formation from the songliao basin, NE China. *Appl. Sci.* 13 (7), 13074295. doi:10.3390/app13074295

Dowey, P. J., and Taylor, K. G. (2020). Diagenetic mineral development within the upper jurassic haynesville-bossier shale, USA. *Sedimentology* 67, 47–77. doi:10.1111/sed.12624

Fan, C., Li, H., Qin, Q., He, S., and Zhang, C. (2020). Geological conditions and exploration potential of shale gas reservoir in Wufeng and Longmaxi Formation of southeastern Sichuan Basin, China. *J. Petroleum Sci. Eng.* 191, 107138. doi:10.1016/j.petrol.2020.107138

Fan, C., Nie, S., Radwan, A. E., Pan, Q., Shi, X., Li, J., et al. (2024). Quantitative prediction and spatial analysis of structural fractures in deep shale gas reservoirs within complex structural zones: a case study of the Longmaxi Formation in the Luzhou area, southern Sichuan Basin, China. *Asian Earth Sci.* 263, 106025. doi:10.1016/j.jseaes.2024.106025

Feng, G., and Chen, S. (1988). Relationship between the reflectance of bitumen and vitrinite in rock. *Nat. Gas. Ind.* 8 (3), 20–25.

Guo, X., Liu, R., Xu, S., Feng, P., Wen, T., and Zhang, T. (2022). Structural deformation of shale pores in the fold-thrust belt: the wufeng-longmaxi shale in the anchang syncline of central Yangtze block. *Adv. Geo-Energy Res.* 6 (6), 515–530. doi:10.46690/ager.2022.06.08

Hackley, P. C., Zhang, T., Jubb, A. M., Valentine, B. J., Dulong, F. T., and Hatcherian, J. J. (2020). Organic petrography of Leonardian (Wolfcamp A) mudrocks and carbonates, Midland Basin, Texas: the fate of oil-prone sedimentary organic matter in the oil window. *Mar. Pet. Geol.* 112, 104086. doi:10.1016/j.marpetgeo.2019.104086

Hu, Z., Wang, R., Liu, Z., Liu, G., Feng, D., Yang, Z., et al. (2021). Source-reservoir characteristics and coupling evaluations for the Lower Jurassic lacustrine shale gas reservoir in the Sichuan Basin. *Earth Sci. Front.* 28 (1), 261–272. doi:10.13745/j.esf.sf.2020.5.24

Kuila, U., McCarty, D. K., Derkowski, A., Fischer, T. B., Topor, T., and Prasad, M. (2014). Nano-scale texture and porosity of organic matter and clay minerals in organic-rich mudrocks. *Fuel* 135, 359–373. doi:10.1016/j.fuel.2014.06.036

Lai, F., Liu, Y., Zhang, H., Wang, H., Mao, H., and Zhang, G. T. (2022). Fracturing properties model of deep shale gas reservoir based on digital core simulation. *J. China Univ. Petroleum Ed. Nat. Sci.* 46 (05), 1–11. doi:10.3969/j.issn.1673-5005.2022.05.001

Li, H., Zhou, J., Mou, X., Guo, H., Wang, X., An, H., et al. (2022). Pore structure and fractal characteristics of the marine shale of the Longmaxi Formation in the changning area, southern Sichuan Basin, China. *Front. Earth Sci.* 10, 1018274. doi:10.3389/feart.2022.1018274

Liu, D., Guo, J., Pan, Z., Du, W., Zhao, F., Chen, Y., et al. (2021b). Overpressure evolution process in shale gas reservoir: evidence from the fluid inclusions in the fractures of Wufeng Formation-Longmaxi Formation in the southern Sichuan Basin. *Nat. Gas. Ind.* 41 (09), 12–22. doi:10.3787/j.issn.1000-0976.2021.09.002

Liu, W., Yu, L., Zhang, W., Fan, M., and Bao, F. (2016). Micro-pore structure of Longmaxi shale from southeast Sichuan Basin. *Mar. Geol. Quat. Geol.* 36 (3), 127–134. doi:10.16562/j.cnki.0256-1492.2016.03.012

Liu, Y., Lai, F., Zhang, H., Tan, Z., Wang, Y., Zhao, X., et al. (2021a). A novel mineral composition inversion method of deep shale gas reservoir in Western Chongqing. *J. Petroleum Sci. Eng.* 202, 108528. doi:10.1016/j.petrol.2021.108528

Milliken, K. L., Rudnicki, M., Awwiller, D. N., and Zhang, T. (2013). Organic matter-hosted pore system, Marcellus formation (Devonian), Pennsylvania. *AAPG Bull.* 97, 177–200. doi:10.1306/07231212048

Mosher, K., He, J., Liu, Y., Rupp, R., and Wilcox, J. (2013). Molecular simulation of methane adsorption in micro- and mesoporous carbons with applications to coal and gas shale systems. *Int. J. Coal Geol.* 109-110, 36–44. doi:10.1016/j.coal.2013.01.001

Shi, Z., Wang, H., Zhao, S., Zhou, T., Zhao, Q., and Qi, N. (2023). Rapid transgressive shale characteristics and organic matter distribution of the upper ordovician-lower silurian wufeng-longmaxi formations in southern Sichuan Basin, China. *J. Palaeogeogr. Chin. Ed.* 25 (04), 788–805. doi:10.7605/gdlxb.2023.04.065

Sing, K. S. W. (1985). Reporting physisorption data for gas/solid systems with special reference to the determination of surface area and porosity (Recommendations 1984). *Pure Appl. Chem.* 57 (4), 603–619. doi:10.1351/pac198557040603

Sun, M., Wen, J., Pan, Z., Liu, B., Blach, T. P., Ji, Y. P., et al. (2022a). Pore accessibility by wettable fluids in overmature marine shales of China: investigations from contrast-matching small-angle neutron scattering (CM-SANS). *Int. J. Coal Geol.* 255, 103987. doi:10.1016/j.coal.2022.103987

Sun, Y., Ju, Y., Zhou, W., Qiao, P., Tao, L., and Xiao, L. (2022b). Nanoscale pore and crack evolution in shear thin layers of shales and the shale gas reservoir effect. *Adv. Geo-Energy Res.* 6 (3), 221–229. doi:10.46690/ager.2022.03.05

Vernik, L., and Landis, C. (1996). Elastic anisotropy of source rocks: implications for hydrocarbon generation and primary migration. *AAPG Bull.* 80 (4), 531–544. doi:10.1306/64ED8836-1724-11D7-8645000102C1865D

Wang, R., Ding, W., Gong, D., Leng, J., Wang, X., Yin, S., et al. (2016). Gas preservation conditions of marine shale in northern Guizhou area: a case study of the Lower Cambrian Niutitang Formation in the Cen'gong block, Guizhou Province. *Oil Gas Geol.* 37 (1), 45–55. doi:10.11743/ogg20160107

Wang, R., Gong, D., Leng, J., Cong, S., Ding, W., Fu, F., et al. (2017). Developmental characteristics of the Lower Cambrian Niutitang shale reservoir in Northern Guizhou area: a case study in the Cengong block. *Earth Sci. Front.* 24 (06), 286–299. doi:10.13745/j.esf.yx.2017-10-4

Wang, R., Hu, Z., Dong, L., Gao, B., Sun, C., Yang, T., et al. (2021a). Advancement and trends of shale gas reservoir characterization and evaluation. *Oil Gas Geol.* 42 (1), 54–65. doi:10.11743/ogg20210105

Wang, R., Hu, Z., Lai, F., Liu, Y., Wu, Z., He, J., et al. (2023a). Resolution of secondary hyperparathyroidism after kidney transplantation and the effect on graft survival. *Oil Gas Geol.* 44 (02), 366–375. doi:10.1097/SLA.0000000000005946

Wang, R., Hu, Z., Long, S., Du, W., Wu, J., Wu, Z., et al. (2022). Comparison of risk scoring systems for upper gastrointestinal bleeding in patients after renal transplantation: a retrospective observational study in Hunan, China. *Oil Gas Geol.* 43 (2), 353–364. doi:10.1186/s12876-022-02426-3

Wang, R., Hu, Z., Sun, C., Liu, Z., Zhang, C., Gao, B., et al. (2018). Comparative analysis of shale reservoir characteristics in the Wufeng-Longmaxi (O_3w-S_1l) and Niutitang ($\in_1 n$) Formations: a case study of wells JY1 and TX1 in the southeastern Sichuan Basin and its neighboring areas, southwestern China. *Interpretation* 6 (4), 31–45. doi:10.1190/INT-2018-0024.1

Wang, R., Hu, Z., Zhou, T., Bao, H., Wu, J., Du, W., et al. (2021b). Characteristics of fractures and their significance for reservoirs in Wufeng Longmaxi shale, Sichuan Basin and its periphery. *Oil Gas Geol.* 42 (6), 1295–1306. doi:10.11743/ogg20210605

Wang, R., Wang, G., Zhao, G., Qian, M., Liu, Y., He, W., et al. (2023b). Geological characteristics and resources potential of shale oil in chang 7 member of upper triassic yanchang Formation in fuxian area, southern ordos basin, western China. *Unconv. Resour.* 3 (1), 237–247. doi:10.1016/j.uncres.2023.06.001

Wei, H., Feng, Q., Yu, J., and Shan, C. (2022). Characteristics and sources of organic matter from the early cambrian Niutitang formtion and its preservation environment in Guizhou. *J. Earth Sci.* 33 (4), 933–944. doi:10.1007/s12583-020-1371-1

Wu, Z., Wang, S., Chen, J., Song, H., Wang, W., Wang, R., et al. (2022). Fracture propagation modes of lower cambrian shale filled with different quartz contents under seepage-stress coupling. *Geofluids* 2022, 1–18. doi:10.1155/2022/1051284

Xu, H., Zhou, W., Hu, Q., Yi, T., Ke, J., Zhao, A., et al. (2021). Quartz types, silica sources and their implications for porosity evolution and rock mechanics in the Paleozoic Longmaxi Formation shale, Sichuan Basin. *Mar. Petroleum Geol.* 128, 105036. doi:10.1016/j.marpetgeo.2021.105036

Yang, R., He, S., Hu, Q., Hu, D., Zhang, S., and Yi, J. (2016). Pore characterization and methane sorption capacity of over-mature organic-rich Wufeng and Longmaxi shales in the southeast Sichuan Basin, China. *Mar. Petroleum Geol.* 77 (11), 247–261. doi:10.1016/j.marpetgeo.2016.06.001

Yang, Z., Fan, M., Tao, C., Lu, L., and Qiang, M. (2022). Carbon isotope fractionation characteristics and significance of black shale desorded gas from Longmaxi Formation in Jiaoshiba area, Sichuan Basin. *Nat. Gas. Geosci.* 33 (8), 1295–1303. doi:10.11764/j.issn.1672-1926.2022.03.006

Zhang, K., Song, Y., Jia, C., Jiang, Z., Han, F., Wang, P., et al. (2022). Formation mechanism of the sealing capacity of the roof and floor strata of marine organic-rich shale and shale itself, and its influence on the characteristics of shale gas and organic matter pore development. *Mar. Petroleum Geol.* 140, 105647. doi:10.1016/j.marpetgeo.2022.105647

Zhang, Q., Liang, F., Liang, P., Zhou, S., Guo, W., Guo, W., et al. (2020). Investigation of fractal characteristics and its main controlling factors of shale reservoir: a case study of the Longmaxi shale in Weiyuan shale gas field. *J. China Univ. Min. Technol.* 49 (1), 110–122. doi:10.13247/j.cnki.jcumt.001068

Zhu, H., Ju, Y., Huang, C., Qi, Y., Ju, L., Yu, K., et al. (2019). Petrophysical properties of the major marine shales in the Upper Yangtze Block, south China: a function of structural deformation. *Mar. Petroleum Geol.* 110, 768–786. doi:10.1016/j.marpetgeo.2019.08.003